# Luminescent Decay of Localized Optical Excitations in KCl*

HERBERT MAHR
*Laboratory of Atomic and Solid State Physics, Department of Physics, Cornell University, Ithaca, New York*

(Received 11 February 1963)

As part of an effort to study absorption, luminescence, and thermal excitation with the same simple impurity system in a KCl single crystal, the luminescence arising from the optical excitation of iodine ions in KCl was measured. The excitation and emission spectra and the yield curves were determined in detail for different concentrations of iodine in the lattice between helium and room temperature and for various exciting photon energies. Results obtained for the thermal broadening of the emission bands, as well as previous results on the thermal broadening of absorption bands can be understood in terms of a simple Franck-Condon model. The existence of 3 emission bands, the observed large Stokes shift, and widely different half-widths of the bands suggest that different excited states are involved in the absorption and emission processes.

## INTRODUCTION

THE absorption of ultraviolet light at impurity ions diluted in an alkali halide lattice leads to well-defined optical spectra which consist of one or more broad bands. Any description of these electronic transitions in ionic crystals has to take into account the strong interaction with lattice vibrations, that is, the strong influence of the instantaneous state of the surrounding ions in the lattice. When this is done, however, a major difficulty arises in describing bound excited states in ionic crystals because of a situation which is unique to those crystals. Any change of the charge distribution of electrons due to the absorption of ultraviolet light influences the equilibrium distribution of the surrounding ions through Coulomb forces. The absorption of light introduces, therefore, a local disturbance in the lattice, in a time short compared to lattice vibrations, before the system can adjust to the new situation and reach thermal equilibrium. Not much is known about the state of the system in the intermediate time interval.

Only after equilibrium is reached does the return of the system from its new excited state to the ground state manifest itself through observable quantities: Luminescence or nonradiative transitions through thermal excitation. A correlation of measurements of excitation and decay will therefore yield information about the local disturbances introduced in the lattice by absorption of light and about the new equilibrium states reached thereafter.

The luminescence measurements which shall be reported in this paper are part of an effort to study absorption, luminescence, and thermal excitation in one and the same simple impurity system with the aim of understanding the processes following an optical excitation. The system used was obtained by diluting a small concentration of iodine ions in a KCl lattice. Detailed measurements of the absorption characteristics of this system have been reported.[1] Localized excitations, or as we may call them, localized excitons are formed at iodine ion sites. These localized excitons are very similar in many of their characteristics to excitons in pure alkali halides which are difficult to study experimentally. For this reason the KI/KCl system is of particular interest.

It was concluded from the absorption measurements that KI/KCl forms a stable solid solution up to a KI concentration of 0.1 mole %. The iodine concentration can be controlled at will and single crystals can be easily grown. The characteristics of the absorption are known over a range of $4\frac{1}{2}$ orders of magnitude of absorption constant and for all practical temperatures and impurity concentrations.[1]

## MEASUREMENTS

KCl single crystals were grown from chlorine treated KCl powder (Mallinckrodt Chemical Company) in a Kyropolous furnace. Small pieces of KI single crystals were added to the melt, the iodine concentration in the crystals being determined by the colorimetric chemical analysis described previously.[1,2] Most of the crystals used in the luminescent measurements contained about $2\times10^{19}$ and $2\times10^{18}$ iodine ions/cc.

A schematic description of the setup used for the excitation and emission measurements is shown in Fig. 1.

For the excitation measurements a vacuum grating monochromator[3] of 1-m focal length dispersed the radiation from an $H_2$-discharge lamp.[4] The pass band of the monochromator was held constant and was about 3 Å for all measurements. Monochromatic radiation from the exit slit could then be passed alternatively onto the crystal sample or onto a sodium salicylate phosphor. This was achieved by rotating the cryostat with the crystal holder through 90°. The sodium salicylate phosphor monitors the intensity of the incident radiation. Luminescent radiation from the sample

* Work supported by the Office of Naval Research and the Advanced Research Projects Agency.

[1] H. Mahr, Phys. Rev. **125**, 1510 (1962); K. Nakamura, K. Fukunda, R. Kato, A. Matsui, and Y. Uchida, J. Phys. Soc. Japan **16**, 1262 (1961).

[2] F. G. Houston, Ann. Chem. **22**, 493 (1950).

[3] P. L. Hartman, Rev. Sci. Instr. **33**, 1082 (1962).

[4] P. L. Hartman and J. R. Nelson, J. Opt. Soc. Am. **47**, 646 (1957); P. L. Hartman, *ibid.* **51**, 113 (1961).

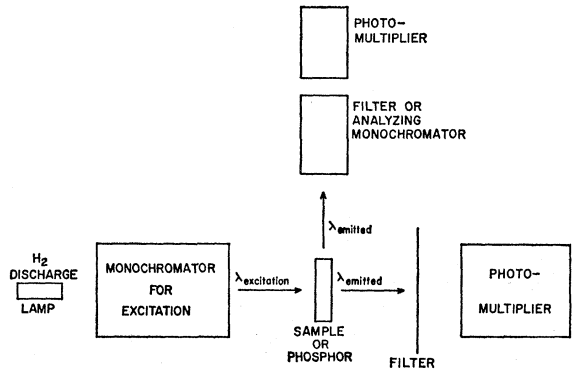


FIG. 1. Experimental setup used for the measurement of the excitation and emission spectra. The monochromator used for excitation was either a vacuum uv grating monochromator or a Bausch and Lomb quartz prism monochromator. The analyzing monochromator was a Bausch and Lomb grating monochromator.

could be detected either in the direction of or perpendicular to the incident beam. For the excitation measurements a spectral range, covering about the spectral width of an emission band was selected either by a nonluminescent Corning No. 3-75 cutoff filter in combination with the red cutoff of a low-dark current EMI photomultiplier 6097S, or by Baird-Atomic uv interference filters. Radiation emitted into the solid angle interrupted by the photomultiplier is then a relative measure of the total number of photons/sec emitted into this spectral range by either sample or reference phosphor. The luminescent yield of the sodium salicylate phosphor is independent of the photon energy in the range over which measurements were made.[5] The ratio of signals obtained from sample and sodium salicylate phosphor is therefore a relative measure of the total luminescence, defined as:

$$\text{Total luminescence} = \frac{\text{Number of photons emitted into an entire emission band/sec}}{\text{Number of incident photons/sec}}.$$

The total luminescence, as the ratio of directly measurable quantities, is widely used in characterizing a luminescent process. For the interpretation of the elementary process of luminescence the total luminescence is not too useful unless the experimental conditions under which the measurements were taken are explicitly stated in each case. Of more direct physical significance is the quantum yield, defined as:

$$\text{Quantum yield } \eta = \frac{\text{Number of photons emitted into an emission band/sec}}{\text{Number of absorbed photons/sec}}.$$

In our case we may neglect reflection losses occurring in sample or reference phosphor. For optically thick crystals ($Kd \gg 1$) the measured total luminescence is then directly equal to the quantum yield $\eta$. For very low values of the absorption constant $K$, however, the sample thickness $d$ simply cannot be chosen large enough. Due to this experimental difficulty the total luminescence in these optically thin samples is now the product of "quantum yield×absorption constant $K$." The quantum yield can then only be determined after dividing the observed luminescence by the absorption constant which was otherwise determined. If the absorption constant is a very rapidly varying function of the photon energy, this correction might introduce large errors. It was attempted in this experiment to set the experimental conditions such that the quantum yield was obtained directly. It will be stated in all cases where the sample could not be made optically thick.

Absolute values of quantum yield and total luminescence were obtained after correcting for the efficiency of the phosphor and the difference in the sensitivity of the detecting system to the different spectral distribution of crystal and phosphor emission.[6] These corrections are only approximately known and the absolute values given in the graphs are certainly only correct within a factor of two.

For the measurement of the emission spectra with *vacuum* uv excitation the emitted radiation was analyzed by a Bausch and Lomb grating monochromator placed perpendicular to the incident beam. For this purpose the bandpass of the dispersing vacuum monochromator was set at about 75 Å.

For the emission measurements (Fig. 1) a Quartz prism monochromator (Bausch and Lomb) dispersed the light from a Nestor Hydrogen Lamp, used and supplied by Cary as the source in their Cary Model 14 spectrophotometer. The wavelength range of the exciting light was then limited by the absorption of air. In some cases the monochromator was flushed with He gas. The monochromatic radiation of a band pass of approximately 100 Å was passed onto the sample, mounted in a cryostat with wide windows. A Bausch and Lomb grating monochromator placed perpendicular to the incident beam analyzed the emitted luminescent radiation. The wavelength band pass was set at either 70 or 35 Å. An EMI photomultiplier 6255S (Quartz envelope) was used to detect the radiation. The recorded spectra were corrected for the spectral response of the photomultiplier and the grating monochromator. As the theoretically predicted band shapes are given for a constant frequency pass band rather than a constant wavelength bandpass, the shape curves for the emission bands were corrected by $(1/\nu^2)d\nu$. In this way a relative

[5] F. S. Johnson, K. Watanabe, and R. Tousey, J. Opt. Soc. Am. 41, 702 (1951).

[6] I am indebted to Dr. T. Timusk for the use of the emission setup and the calibration of the response curves.

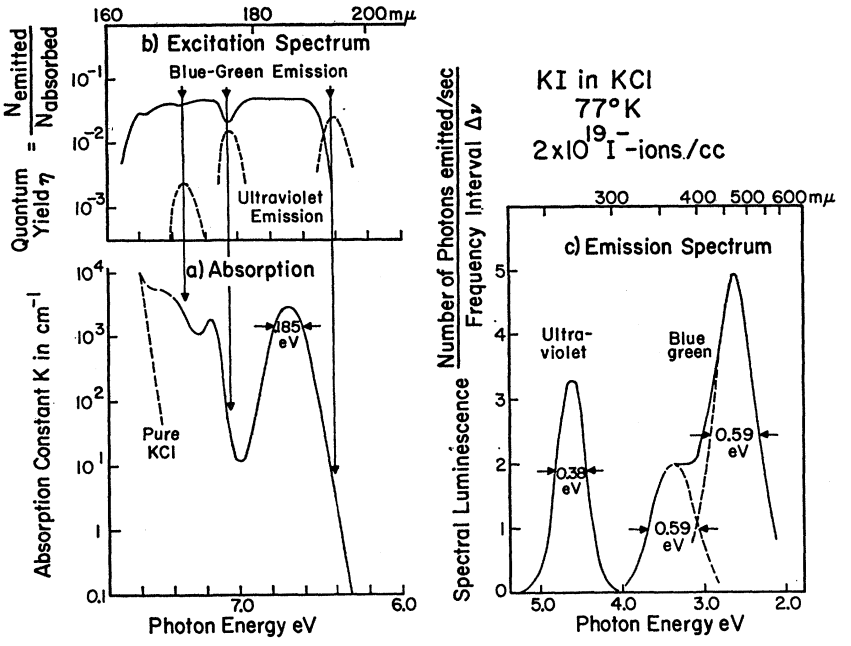


FIG. 2. Optical behavior of $2\times10^{19}$ iodine ions/cc diluted in KCl crystals at 77°K. (a) Absorption spectrum: The absorption constant is plotted on a logarithmic scale vs the photon energy. The dashed line indicates the position of the absorption edge of pure KCl. (b) Excitation spectrum: The solid line represents the quantum yield for the blue-green component of the blue-green emission band. The dashed line shows the three regions of uv emission. These latter curves correspond to uncorrected values of total luminescence. The arrows point at coincident positions of a depression in the yield curve of the blue-green component emission, of excitation maxima for the uv emission and regions on the low-energy tail of the three absorption bands. (c) Emission spectrum: The spectral luminescence (arbitrary units) of the uv and the blue-green emission is plotted vs the photon energy. Note the different scale used for the photon energy. The blue-green emission consists of two components, a large blue-green and a smaller blue emission band.

measure for the spectral luminescence, defined as:

Spectral luminescence

$$=\frac{\text{Number of photons emitted/sec}}{\text{Frequency interval }\Delta\nu}=\frac{N_{\text{emitted}}/\text{sec}}{\Delta\nu}$$

was obtained and plotted in the emission curves vs the photon energy $h\nu$. The spectral response of photomultiplier and monochromator[6] were obtained with a tungsten filament lamp calibrated by the National Bureau of Standards and from a comparison with the constant yield[5] of sodium salicylate at short wavelengths. The incident light intensity was determined from a comparison with the constant quantum yield of sodium salicylate.

## RESULTS

Figure 2 gives a survey of the optical properties of the iodine centers in KCl at 77°K. In Fig. 2(a) the absorption constant on a logarithmic scale is plotted vs the photon energy. Two absorption bands are clearly resolved, a third one is indicated. The dashed line at higher energies corresponds to the absorption edge of pure KCl. Illumination in the iodine absorption bands gives rise to a blue-green luminescence of characteristics shown on the right in Fig. 2(c). Here the spectral luminescence in relative units is plotted on a linear scale against the photon energy. The scale of the photon energy is doubled from that used in the absorption plot. The blue-green emission has two overlapping components, a large blue-green band with the maximum at 2.64 eV and a smaller blue band with the maximum at 3.4 eV at 77°K. The total area under these curves is a relative measure of the total luminescence which is equal to the quantum yield for the optically thick crystals used in these experiments. From emission bands obtained under excitation with different photon energies the quantum yield was obtained as a function of exciting photon energy and is plotted above the absorption graph in Fig. 2(b). The yield for the blue-green component is roughly constant throughout the range of iodine absorption as shown by the solid line. There are, however, three regions, indicated by arrows, where the yield is depressed. This depression is very clear for the dip in the middle. At low-photon energies the depression is indicated by a nonsymmetric behavior of the yield compared to the peak of the low-energy absorption

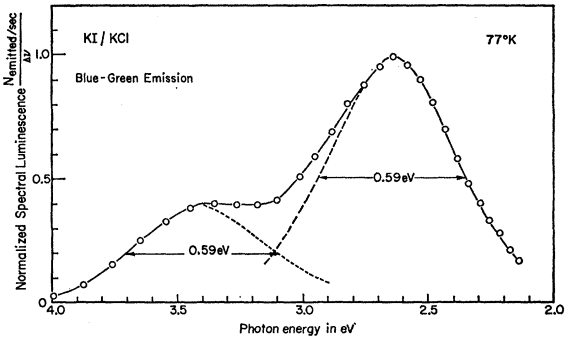


FIG. 3. The two overlapping components of the blue-green emission measured at 77°K. From the shape of the undisturbed sides a symmetric form was constructed, as indicated by the dashed lines. The data points shown were obtained from measurements taken at various exciting photon energies throughout the range of iodine absorption and with samples containing $10^{18}$ and $10^{19}$ iodine ions/cc. The half-width is the same for both components.

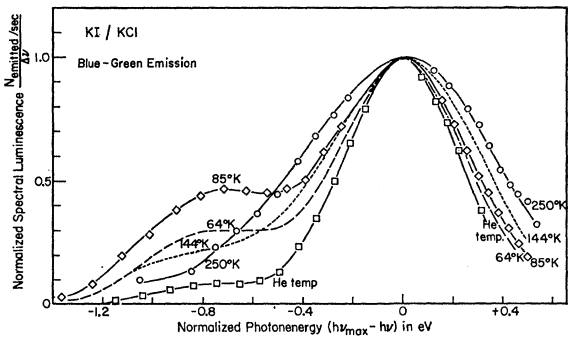


FIG. 4. Normalized shape curves of the blue-green emission bands at various temperatures. Data points are from measurements taken at various exciting photon energies throughout the iodine absorption and for samples containing $10^{18}$ and $10^{19}$ iodine ions/cc.

band. This depression does not recover towards low energies because the sample then becomes optically thin and the measured signal follows the rapid decrease of the absorption constant. The high-energy depression is only slightly seen in the graph but is clearly reproducible.

Excitation in any of these regions leads also to the emission of an ultraviolet band. Its spectral luminescence is shown in Fig. 2(c) with a maximum at 4.64 eV at 77°K. The total luminescence emitted into this uv band is given by the dashed line in the graph of the excitation spectrum Fig. 2(b). The maxima of the observed total luminescence coincide with the depressions that occur in the yield curve for the blue-green emission. Furthermore, the regions of maximum emission of uv light coincide with regions on the low-energy tail of the absorption bands in all three cases, as indicated by arrows.

## Emission Spectra

In the following two sections the results obtained for the emission and excitation spectra are discussed in more detail. Figure 3 shows a detailed measurement of the blue-green emission bands at 77°K. Identical points were obtained with two samples of different iodine concentrations ($2\times10^{19}$ and $2\times10^{18}$ iodine ions/cc) and with various energy values of the exciting light. There is no change in the shape of the emission band with iodine concentration or exciting wavelength throughout the region of iodine absorption. The data points of Fig. 3 were obtained with a resolution of 70 Å. Control runs taken with 35 and 17.5 Å resolution showed that the resolution was sufficient. From the shape of the undisturbed sides of the two overlapping emission bands a symmetric form was constructed for both bands as shown by the dashed lines. This procedure was found to be consistent with the shapes at higher temperatures where the small band is almost absent. From this analysis reliable values for the half-width of the bands were obtained.

Figure 4 shows the temperature dependence of the two blue-green emission bands. The spectral luminescence, normalized to unity at the peak of the large blue-green component, is plotted vs the normalized photon energy ($h\nu_{max}-h\nu$), where $\nu_{max}$ is the frequency at the band peak. The most striking feature is the change in relative height of the small emission band. From a very small value at He temperature the height rises to a maximum in the vicinity of 100°K and falls off towards room temperature. The half-width of the large band increases monotonically with temperature as can be seen at the low-energy tail. Figure 5 shows similar normalized shape curves of the uv emission as a function of temperature. The measurements were taken with a resolution of 35 Å. Again the shapes of the curves were found to be the same for excitation in any of the three regions of exciting photon energy which stimulate this emission. The values of the half-width obtained as a function of temperature are presented in Fig. 7.

Figure 6 shows the change of the maximum position of the uv emission as a function of temperature (left-hand ordinate scale). For comparison, the change of the maximum position of the low-energy absorption band with temperature is included (right-hand scale). For higher temperatures $h\nu_{max}$ varies nearly linearly with $T$ in both cases, but approaches a constant value at low temperatures.

The change of the half-width of the emission bands with temperature is shown in Fig. 7. The square of the half-width is plotted vs the temperature, the left-hand scale corresponding to the emission bands, the right-hand scale to $H^2$, the square of the half-width of the low-energy absorption band. At high temperatures $H^2$ is proportional to the temperature $T$ in all three cases; at low temperatures the half-widths level off towards a constant value at 0°K. The ordinate scale used for plotting the absorption results (right-hand scale) was multiplied by a factor 10. In this way, a common curve could be traced through the data points obtained from both the absorption band and the blue-green emission band in question. For the uv emission the half-width is

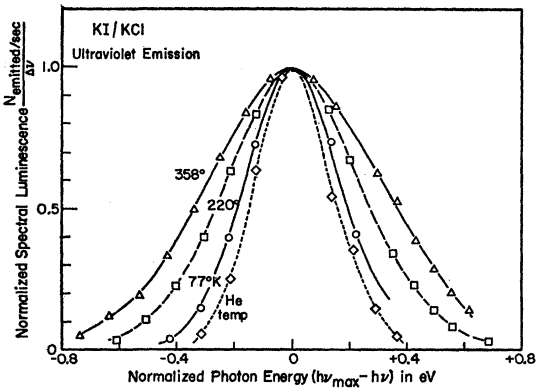


FIG. 5. Normalized shape curves of the uv emission band at various temperatures.

given as measured by the solid circles. The open circles are the same values multiplied by a common factor of 2.43. Within the accuracy of the determination of the half-width, the temperature variation of the half-widths is the same in all three cases. At all temperatures where the smaller blue component of the blue-green emission is prominent enough, its half-width (determined as shown in Fig. 3) was approximately the same as the one obtained for the larger band. The absolute values of the half-widths for the various bands are like 1:1.56:3.16 for the low energy absorption band, the ultraviolet emission band, and the two blue-green emission bands, respectively. The shape of the emission bands was obtained after correcting for the spectral response of the analyzing grating monochromator and the photomultiplier. Also, the intensity as recorded at constant slit width, that is, at constant wavelength interval $\Delta\lambda$, was converted to the number of photons/constant frequency interval $\Delta\nu$. Slight asymmetries and errors are likely, and a more rigorous analysis of the shape curves was not attempted. Approximately, however, the shape is Gaussian.

## Excitation Spectra

Figure 8 shows a more detailed analysis of the excitation spectra. The total luminescence is plotted vs the photon energy of the incident uv light. The data points correspond to samples with the two different iodine concentrations. For very thick crystals and in regions of high-absorption constants all the incident quanta are absorbed, neglecting reflection losses. In Fig. 8, the solid curve at the top shows the variation of the quantum yield with exciting energy for the blue-green component of this emission for thick crystals. The dashed line connects data points obtained from an optically thin sample. The relative number of absorbed photons/sec is then proportional to the number of incident photons/sec times the absorption constant. Therefore, the total luminescence found in this case should reflect the shape of the absorption constant. The arrows indicate the position of the two resolved absorption bands [Fig. 2(a)] which coincide with the maximum luminescence found. The results obtained with the blue-green component of the blue-green emission for optically thin samples thus confirm the absorption measurements. The highest energy absorption peak is even better resolved in emission as shown by comparison with the peaks in Fig. 2.

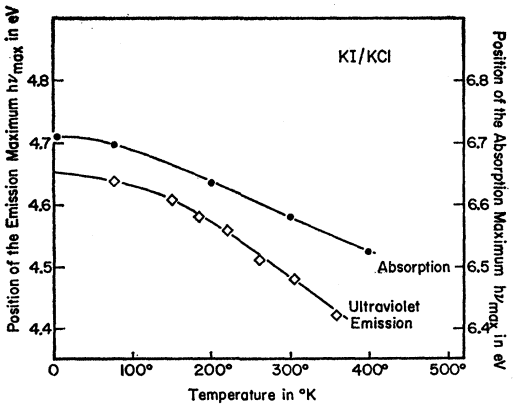


FIG. 6. The position of the emission band and absorption band maxima as a function of sample temperature. The left-hand ordinate scale corresponds to the values obtained from the uv emission band; the right-hand ordinate scale shows the position (obtained from measurements) of the low-energy absorption band.

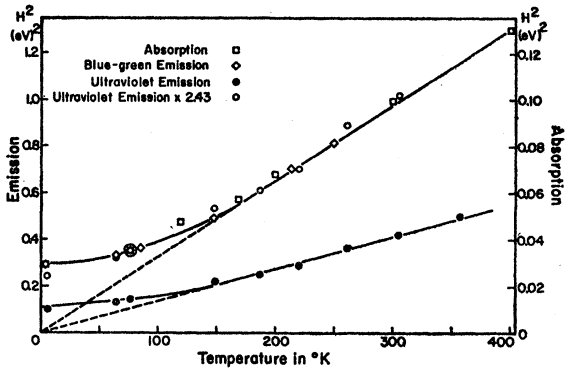


FIG. 7. Temperature dependence of the half-widths of the emission bands and the low-energy absorption band: The left ordinate scale corresponds to values of the blue-green and uv emission bands, the right-hand ordinate scale corresponds to values obtained from the low-energy absorption band. Both scales measure the square of the half-widths. The open circles represent the measured values of the square of the half-widths of the uv emission multiplied by a common factor 2.43.

The excitation spectrum for the uv emission is given by the dotted line in Fig. 8. This emission can be excited appreciably in crystals which are 1–2 mm thick and contain large iodine concentrations. The excitation spectrum of this emission has three maxima which coincide with the depressions found in the yield curve of the blue-green component of the blue-green emission. The three maxima also coincide with regions on the low energy tail of the absorption bands; there is no emission of uv light at correspondingly low-absorption levels at the high-energy side of the absorption bands (compare Fig. 8 with Fig. 2).

Due to the very rapid decrease of the absorption constant at the low-energy tail of the absorption bands even the thickest crystals containing $10^{19}$ iodine ions/cc were still optically thin over part of the low-energy side of each excitation region. The aperture of the grating monochromator limited the sample thickness to values of about 2 mm. This experimental difficulty makes the interpretation of the shape of the excitation curves difficult. At the maxima of the excitation peaks 100% of the incident light intensity is absorbed. Each excitation curve is therefore characteristic of a quantum yield on the high-energy side of the excitation maxima. On the low-energy side less and less light is absorbed, and therefore the measured values of the total luminescence emitted give only the product of $\eta \times K$ in that region.

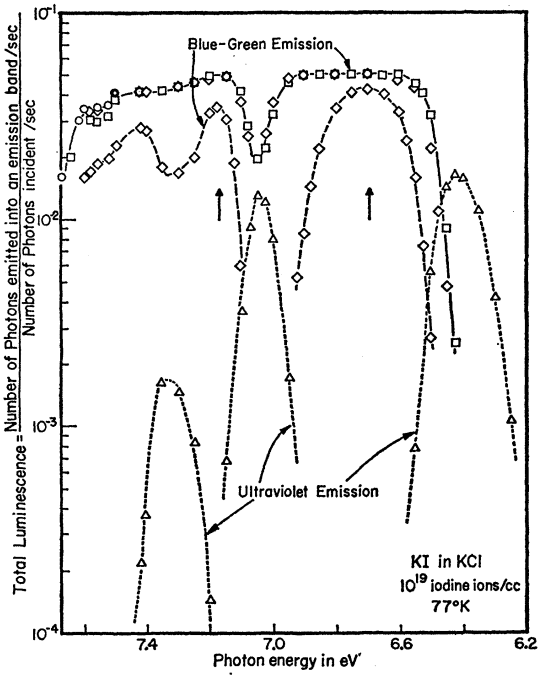


FIG. 8. Excitation spectra for optically thick and optically thin samples: The solid line connects measurements from an optically thick sample ($d=3$ mm) and measures the quantum yield of the blue-green component of the blue-green emission. The data connected by the dashed line were obtained from an optically thin sample ($d\approx 10\ \mu$) where the measured total luminescence represents the spectral dependence of the absorption constant. The dotted line connects data obtained from a 2-mm-thick sample and represents the excitation spectrum of the uv emission band. In each of the three regions the sample is optically thick on the high-energy side and optically thin at the low-energy side.

If the quantum yield is constant to the low-energy side of each excitation maximum then the curves reflect the shape of the absorption constant.

Figure 9 shows the temperature dependence of the quantum yield for the three emission bands. The values were obtained in different ways. One set of data points corresponds to measuring the total number of emitted photons by selecting the band pass with cutoff and interference filters. In another set of measurements the quantum yield was obtained from the integrated area of the emission bands (Figs. 4 and 5). Both sets of data points agree well. Two different iodine concentrations and various exciting wavelengths were used. The temperature dependence of the quantum yield was found in all cases to be independent of concentration or exciting photon energy within the iodine absorption band.

The most accurate set of data was obtained for the large blue-green component of the blue-green emission bands. The yield is constant from 60 to about 150°K and falls off very rapidly towards room temperature. The yield of the smaller blue component of the blue-green emission could be measured with accuracy only in a small temperature range where its relative height is large enough. At liquid-helium temperature the yield starts at a low value of approximately $(2\text{–}3)\times 10^{-3}$, rises then to a maximum of $2\times 10^{-2}$ at around 100°K and then falls off. Because of the overlap of the large blue-green emission the lowest values of the yield could not be very well determined. The situation is worse for the quantum yield of the ultraviolet emission. The low-energy tail of the absorption band, in which region this emission is excited, shifts with temperature and the tail becomes much less steep at higher temperatures. Consequently, it is difficult to determine how much light is really absorbed at different temperatures in the region where uv emission is stimulated. In Fig. 9 measurements obtained from a thick sample of the highest iodine concentration are reproduced. At around 200°K the yield drops very rapidly from an approximately constant value at lower temperatures.

## DISCUSSION

### Summary of the Results

For the discussion of the results some of the observations are summarized, including results obtained for the absorption of iodine in KCl.[1]

(1) Position and half-width of the two absorption bands are independent of the iodine concentration up to $2\times 10^{19}$ iodine ions/cc. The total integrated area of the absorption band $\int Kd(h\nu)$ is proportional to the iodine concentration. The shape of the absorption band is Gaussian near the maximum absorption; the absorption constant follows Urbach's rule at low absorption levels at the low-energy side. No changes were found in the results of absorption measurements with the same crystal over a period of two years and no

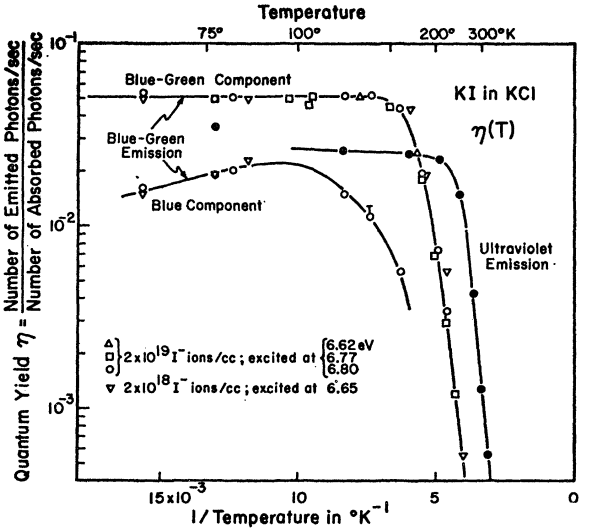


FIG. 9. Temperature dependence of the quantum yield: The temperature dependence of the quantum yield of the blue-green emission bands was obtained at various exciting photon energies for $2\times 10^{19}$ and $2\times 10^{18}$ iodine ions/cc, respectively. The data for the uv emission (full circles) were obtained from a 2-mm-thick sample containing $2\times 10^{19}$ iodine ions/cc. The sample was only approximately optically thick for the exciting light at various temperatures.

colloidal bands or other absorption bands could be detected at higher wavelengths out to the infrared reststrahlen absorption of KCl.

These results then suggest the following conclusions: (a) Diluted iodine ions in KCl single crystals occupy substitutionally $Cl^-$ sites and are stable impurities at room temperature. They are atomically dispersed. (b) There is little or no interaction between neighboring centers up to concentrations of $2\times10^{19}$ iodine ions/cc.

The position of the long-wavelength absorption band is shifted from the position of the exciton band of pure KI by an amount which can be understood in terms of a different lattice constant of the surrounding lattice. We might, therefore, attribute the iodine absorption to the formation of excitons at iodine sites in KCl.

(2) The half-widths of absorption and emission bands vary over a wide range. At 77°K the half-widths are: low-energy absorption band, $H=0.185$ eV; high-energy absorption band, $H\approx0.09$ eV; blue-green emission band, $H=0.59$ eV; ultraviolet emission band, $H=0.38$ eV. The temperature dependence of the half-widths of absorption and emission bands is, however, the same.

(3) The Stokes shift $\Delta E_s$ of the emission bands is very large:

| | Ultraviolet band (eV) | Small blue band (eV) | Large blue-green band (eV) |
|---|---|---|---|
| $h\nu_{max}$ | 4.64 | 3.4 | 2.64 |
| $\Delta E_s$ | 2.06 | 3.3 | 4.06 |

(4) The temperature dependence of the quantum yield and the shape of the emission bands were found to be independent of the exciting photon energy. This suggests that after the absorption process thermal equilibrium is reached before re-emission takes place.

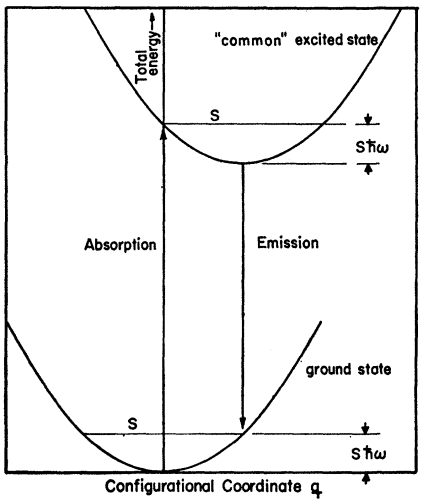


FIG. 10. One-coordinate-configurational (C.C.) Franck-Condon model. The total energy of the impurity system is plotted vs the configurational coordinate $q$. Transitions corresponding to maximum absorption and maximum emission are indicated. These transitions lead to vibrational levels $S$. This special model assumes a "common" excited state for absorption and emission process.

This is reasonable because the radiative decay time of $10^{-8}$ sec or longer is orders of magnitude longer than the reciprocal of most lattice frequencies.

(5) The uv emission is excited in three regions which, in all cases, cover ranges of absorption constants on the low energy tail of the absorption bands.

## Franck-Condon Model

The thermal broadening of absorption and emission lines in ionic solids is usually discussed in terms of a Franck-Condon model.[7] For comparison with experimental data the Franck-Condon picture is often used in its simplest form, as a one-configurational-coordinate (C.C.) model. This C.C. model assumes that a single lattice vibration of suitable eigenvector $q$ and frequency $\omega$ might replace the effect of many lattice modes on the thermal broadening of an electronic transition. As pointed out by Markham[7] the validity of this assumption can be checked. For the absorption of the $F$ center in KCl this has been done[8] by very carefully measuring the temperature variation of the half-widths. For a rather large number of other impurity systems in alkali halides results of absorption and emission measurements are available. To the extent to which the various authors have measured the exact shape and its temperature variation, all these results are consistent with the prediction of a simple one coordinate Franck-Condon model.

In addition to explaining the thermal broadening of the bands, the Franck-Condon model is also used to connect the emission and absorption processes via a common excited state[9,10] as sketched in Fig. 10. It is the purpose of this discussion to show that the results obtained from the system KI/KCl disagree with those predictions of the simple Franck-Condon model which arise from the coupling of emission and absorption through one and the same excited state. It is shown that recent results obtained from emission studies with other impurity systems in alkali halides by other authors are also not consistent with predictions from this coupling. On the other hand, we want to show that the results reported here are in good agreement with those predictions of the simple C.C. model which result from the description of an individual transition, in emission as well as in absorption.

## Comparison of Theory and Experiment

(a) The specific predictions arising from the assumption of a common excited state, coupling absorption

[7] For references to earlier work and a critical analysis of the theoretical aspects see J. J. Markham, Rev. Mod. Phys. **31**, 956 (1959).

[8] J. D. Konitzer and J. J. Markham, J. Chem. Phys. **32**, 843 (1960).

[9] A. von Hippel, Z. Physik **101**, 680 (1936). F. Seitz, Trans. Faraday Soc. **35**, 79 (1939).

[10] C. C. Klick and J. H. Schulman, in *Solid State Physics*, edited by F. Seitz and D. Turnbull (Academic Press Inc., New York, 1957), Vol. 5.

and emission, are (Fig. 10): (1) If the absorption is due to an allowed electronic dipole transition then the emission is also an allowed process. The radiative lifetime of the excited state should then be of the order of $10^{-8}$ sec.[11] (2) If the force constants coupling the surrounding ions in the excited state are not too different from their values in the ground state of the system, the absolute values of the half-width of absorption and emission bands should be about the same. More specifically the model predicts[10]: $H(0)_{\text{Absorption}}/H(0)_{\text{Emission}}=(K_e/K_g)^{5/4}$, where the $H(0)$ are the respective half-widths at zero temperature and $K_e$, $K_g$ the force constants of the excited and ground state. (3) There should be only one emission band. (4) The Stokes shift $\Delta E_s=h\nu_{\max}(\text{Abs})-h\nu_{\max}(\text{Emis})$ is intimately related to other experimental data[10]:

$$\Delta E_s=2S\hbar\omega\approx H^2(0)_{\text{Abs}}/2.5\hbar\omega,$$

where $\omega$ is the frequency of the interacting lattice vibration. For typical values of half-width and frequencies of impurity bands in alkali halides we get: $\Delta E_s\leq 1$ eV.

Results obtained from the KI/KCl system and several recent experiments done by various authors on different impurity systems of alkali halides disagree with one or more of these predictions: (1) Brown and Swank[12] observed the radiative lifetime of the excited $F$ center to be $10^{-6}$ sec, about 100 times larger than the expected value of $10^{-8}$ sec.[11] (2) The half-width of absorption and emission bands of iodine in KCl reported in this work are widely different from each other. Emission bands obtained from excitation of $\alpha$ centers[13] and Tl centers in KCl, KBr, and KI[14] show much larger half-widths than the corresponding absorption bands. (3) Three, rather than one, emission bands were observed for KI/KCl. There are also several emission bands reported in the Tl systems.[14] (4) The Stokes shift of all three emission bands of KI/KCl is much larger than the shift of $\leq 0.7$ eV predicted from the model. The Stokes shift of 4 eV reported for the $\alpha$-center luminescence[13] is also much larger than the model predicts.

(b) For an individual transition between two different electronic states the C.C. model predicts an approximately Gaussian shape of the resulting absorption or emission band[7,15] and a temperature dependence of the half-width of the band which is given by:

$$H^2(T)=H^2(0)\coth(\hbar\omega/2kT),$$
$$\text{with}\quad H^2(0)=5.5S(\hbar\omega)^2. \quad (1)$$

Here $H(T)$ is the measured half-width at temperature $T$, H(0) the half-width at near-zero temperature, $\hbar\omega$ the level spacing of the excited and ground state oscillator and $S$ the vibrational level of the oscillator reached in the peak of the emission or absorption process.

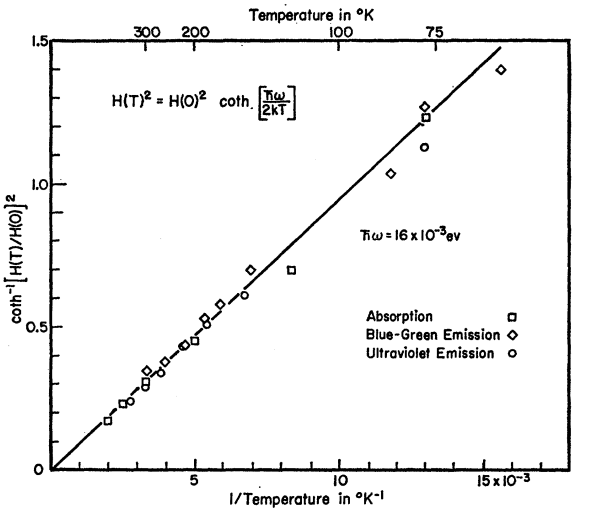


FIG. 11. Values of $\coth^{-1}[H^2(T)/H^2(0)]$, obtained from the measurements of the half-width of the low-energy absorption band, the blue-green component of the blue-green emission bands and of the uv emission band, are plotted vs $1/T$. The slope of the straight line, given by formula (1) corresponds to a value of $\hbar\omega=16\times10^{-3}$ eV.

These predictions agree well with experimental results obtained here. The band shapes are all approximately Gaussian. The measured half-widths of each band are plotted as $\coth^{-1}[H^2(T)/H^2(0)]$ vs the reciprocal of the temperature, $1/T$, in Fig. 11. A straight line, predicted by formula (1) for this particular plot, can be drawn through the results obtained from three different bands, the low-energy absorption band and the two larger emission bands. It might be well to emphasize that the data can, thus, be interpreted with the assumption that only a single lattice vibration of frequency $\omega$ is effective; the data are, however, not good enough to prove that *only* one frequency is operative in all three cases. From the slope of the straight line, which is $\hbar\omega/2k$ one obtains $\hbar\omega=(16\pm1)\times10^{-3}$ eV, or an effective vibrational frequency of $\omega_{\text{eff}}=2\pi\times3.9\times10^{12}$ sec$^{-1}$. This means then that the same effective frequency of lattice vibrations is dominant in determining the widths of the three bands.

## CONCLUSIONS

(a) It was shown in the previous section that the simple C.C. model is successful in describing the experimental results of individual transitions. The combined description of the absorption and the emission process, using a common excited state, leads to predictions which are in disagreement with experimental observations. Experimental results lead to the proposal of an alternative C.C. model which employs different excited states, one reached in the absorption process and other ones where the emission processes originate. Figure 12

[11] J. J. Markham, Bull. Am. Phys. Soc. **7**, 197 (1962). W. Beall Fowler and D. L. Dexter, Phys. Rev. **128**, 2154 (1962).
[12] F. C. Brown and R. K. Swank, Phys. Rev. Letters **8**, 10 (1962).
[13] T. Timusk, Bull. Am. Phys. Soc. **7**, 38 (1962).
[14] R. Edgerton and K. Teegarden, Phys. Rev. **129**, 169 (1963).
[15] M. Wagner, Z. Naturforsch. **15a**, 889 (1960); **16a**, 302 (1961).

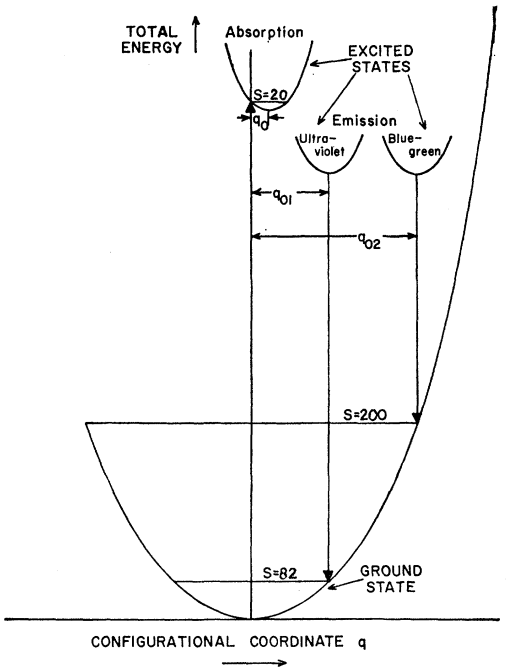


FIG. 12. One-coordinate-configurational Franck-Condon model proposed for the KI/KCl system. It is assumed that different excited states are involved in the absorption and emission processes. An analysis of the individual transitions based on formula (1) gives the values of $S$ and $q_0$ given. The diagram is not drawn to scale.

is a very schematic representation of such a model; it is not drawn to scale.

More specifically we propose the following model: Absorption of light at iodine centers in KCl gives rise to an allowed electric dipole transition. A defined new electronic state is reached (Born-Oppenheimer approximation) and the new electronic wave function stabilized in a time short compared to the reciprocal of lattice vibrational frequencies (Franck-Condon principle). This change of charge distribution of electrons, fast as it is compared to the motion of ions, influences the equilibrium position of the surrounding ions through Coulomb forces. After the excitation takes place the surrounding lattice tends to relax towards these well defined new equilibrium positions by means of lattice vibrations. From the interpretation given to the experimental results we conclude that this equilibrium is not reached. Rather a fraction $k$ of the excited centers occupies finally another excited state with different equilibrium positions of the surrounding ions. This new excited state is in thermal equilibrium with the lattice. Within the lifetime of the new excited state the system decays either by radiation, or by thermal processes which lead the system out of its excited state without emission of radiation.

(b) *Half-width and Stokes Shift.* A detailed analysis of the temperature variation of the half-width of absorption and emission bands, suggested by formula (1), provides numerical values for $S$, $S$ is the vibrational level of the C.C. oscillator model which is reached at the peak of emission or absorption. The values are $S=20$ for the low-energy absorption band, $S=82$ for the uv and $S=200$ for the blue-green emission band. They are included in Fig. 12. This figure makes use of the result that the same lattice frequency $\omega$ interacts with all three transitions. $S$ gives the average number of phonons released after an optical transition. From the values of $S$ the relative equilibrium shifts $q_0$ for the different excited states can be calculated. The shift $q_{02}$ of the excited state from which blue-green emission occurs is 1.56 times as large as the shift $q_{01}$ of the excited state from which ultraviolet emission occurs (Fig. 12). Both equilibrium shifts are different from the shift $q_0$ of the excited state reached in absorption. A straightforward analysis of the individual transitions with a C.C. model leads thus to a result which is consistent with our assumption of different excited states. The Stokes shift is now a parameter which has to be determined experimentally.

(c) *Excitation Spectra.* The shape of the emission bands and the efficiency of emission were found to be independent of the exciting photon energy throughout the range of iodine absorption. This means that the same fraction $k$ of excited centers will always end up in thermal equilibrium with the lattice. $k$ is 0.02–0.05 in the results reported. It does not matter which of the different absorption bands is used for excitations nor, within limits, where, within one absorption band, the excitation takes place. There is, however, a distinct difference between excitations in the low-energy tail of a particular absorption band leading to an excited state from which uv light is emitted, and excitations in the rest of the absorption band leading to a different excited state from which blue-green light is emitted. Certainly a very detailed model is needed to explain these experimental observations. Excited states which cannot be reached by allowed optical transitions from the ground state may play an important role. It is felt that more experimental information is needed, also with other impurity systems, before such a detailed description might be attempted. There are many examples of impurity system where the observed quantum yield is much smaller than one or where luminescence is completely absent ($k=0$). The questions posed by the simple impurity system KI/KCl might, therefore, be of more general interest.

## ACKNOWLEDGMENTS

I wish to express my gratitude to Professor P. L. Hartman for his most valuable help throughout the entire investigation. I also want to thank Professor J. A. Krumhansl, Professor R. H. Silsbee, Dr. M. Wagner, and Dr. T. Timusk for helpful suggestions and discussions, and Professor R. O. Pohl for providing the mixed single crystals. It was especially appreciated that Dr. Timusk's apparatus could be used during this investigation.